AIMS Mathematics

AIMS Mathematics, 11(8): 27327–27350.
DOI: 10.3934/math.20261093
Received: 16 April 2026
Revised: 29 July 2026
Accepted: 30 July 2026
Published: 28 August 2026

https://www.aimspress.com/journal/Math

Research article

Mathematical modeling of an explainable deep learning-based UAV obstacle detection framework using multi-sensor data for urban air mobility systems

Sarah A. Alzakari[1], Shaymaa Sorour[2], Saleh Alghamdi[3], Ahmed Omer Ahmed Ismail[4], Nabil Almashfi[5], Aisha Blfgeh[6], Fahad F. Alruwaili[7,*] and Somia A. Asklany[8]

[1] Department of Computer Sciences, College of Computer and Information Sciences, Princess Nourah bint Abdulrahman University, P.O. Box 84428, Riyadh 11671, Saudi Arabia
[2] Department of Management Information Systems, School of Business, King Faisal University, Al-Ahsa 31982, Saudi Arabia
[3] King Abdulaziz City for Science and Technology, Saudi Arabia
[4] Department of Information Systems, Applied College at Mahayil, King Khalid University, Saudi Arabia
[5] Department of Software Engineering, College of Computer and Information Sciences, Jouf University, Sakaka 72341, Saudi Arabia
[6] Department of Computer Science and Artificial Intelligence, College of Computer Science and Engineering, University of Jeddah, Jeddah, 23890, Saudi Arabia
[7] Department of Computer & Network Engineering, College of Computing and Information Technology, Shaqra University, Sharqa, Saudi Arabia
[8] Department of Computer Science, College of Science, Northern Border University, Arar, Saudi Arabia

* **Correspondence:** Email: alruwaili@su.edu.sa.

Abstract: Autonomous operations are an essential function of urban air mobility (UAM) and other evolving aviation markets. Achieving autonomous flight within complex environments remains a bottleneck in the area of unmanned aerial vehicles (UAVs). Current progress in sensor technology has improved the payload capabilities of UAVs, allowing the incorporation of sensors, namely multispectral cameras, higher spatial resolution cameras, and light detection and ranging (LiDAR) systems. Moreover, the fusion of data from diverse sensor modalities can compensate for the limitations of individual sensors, offering a more comprehensive representation of the operating environment. Thus, a systematic analysis of path optimization methods that employ multi-sensor data fusion is critical for enhancing the autonomy and reliability of UAV systems. At present, scholars have progressively utilized deep learning (DL)-driven systems to overcome these challenges for general object detection tasks and have achieved considerable advancements. However, the application of DL methods specifically for UAV recognition and classification remains a relatively novel research field. This paper presents a novel explainable deep learning-based UAV obstacle detection framework (XDL-UAVODF) using multi-sensor data. The aim of this study is to design a UAV navigation framework for obstacle avoidance and optimal trajectory planning in dynamic and complex environments. Obstacle detection provides fundamental environmental awareness for safe navigation and serves as an essential condition for subsequent path planning and trajectory generation. The proposed approach is designed to support UAV navigation by accurately identifying obstacles rather than directly generating collision-free paths. For feature selection, a hybrid approach that integrates principal component analysis (PCA) and least absolute shrinkage and selection operator (LASSO) is leveraged to reduce dimensionality and select significant feature subsets. Moreover, the dynamic sparse graph convolutional recurrent network (DSGCGRN) is used to model spatial-temporal relationships and analyze complex patterns among multi-sensor data to improve decision-making performance. The AdaGrad optimizer is utilized in the training process to ensure faster convergence and enhance model stability. Finally, SHapley Additive exPlanations (SHAP) is employed to explain feature contributions and enhance the transparency of the deep learning model. The performance validation analysis of the XDL-UAVODF approach is conducted using the UAV Autonomous Navigation Dataset. The experimental outcomes reported the superiority of the XDL-UAVODF technique under various measures.

Keywords: unmanned aerial vehicle; deep learning; principal component analysis; explainable artificial intelligence; urban air mobility

Mathematics Subject Classification: 68T07, 68T45

1. Introduction

Urban air mobility (UAM) facilities are developing airborne missions involving on-demand air taxis in lower-altitude metropolitan areas, last-mile delivery, and scheduled public air metro. Also, the quick iterative procedure of electrical vertical takeoff and landing (eVTOL) aircraft makes it soon possible and suitable for urban air transport [1]. At the same time, frequent flight actions in lower-altitude urban airspace are controlled by security and safety considerations, as the flow of heavy traffic with probable conflicts may endanger the people [2]. Meanwhile, the urban building complexity alters the wind field and microclimate, significantly impacting fleet operation in densely distributed areas. Unmanned aerial vehicles (UAVs) autonomous control is a pivotal research domain because of its numerous applications in logistics, disaster response, environmental observation, and military reconnaissance [3]. As UAVs progressively operate in dynamic and intricate surroundings, the need for extremely effective and consistent path optimization approaches has increased considerably. Conventional navigation approaches frequently struggle with the computational load of real-world decision-making, sensor noise, and environmental uncertainties [4].

UAVs are aircraft that operate under either autonomously piloted or centrally controlled conditions. UAVs are appropriate for a broad range of applications, including commercial, surveillance, defense, and scientific operations [5]. Position tracking, drone mapping, and object monitoring are regular uses for UAVs due to their affordable operating costs, compact size, and capability for vertical landing and takeoff. UAV path planning can be regarded as a procedure in which drones compute a route to reach the target location rapidly and safely, with the plan based on the existing setting and position as key elements [6]. UAVs must maintain full awareness of their status to execute missions efficiently. Examples of their status involve monitoring their position, direct route, destination, reference point, and travel speed [7]. Therefore, multi-UAV functions are a more complex and time-consuming research area, leading to high computational expenses related to a single UAV mission [8].

The latest developments in deep learning (DL) models have resulted in further enhancements in UAV navigation, especially in the interpretation and processing of higher-dimensional sensor information [9]. Deep neural networks (DNNs) include recurrent and convolutional methods that are useful for feature extraction from intricate sensor inputs, allowing UAVs to make more precise and consistent decisions in various systems. Pretrained methods like convolutional autoencoders or transformers enable knowledge transfer across tasks, decreasing the dependence on task-specific databases [10]. These advancements have significantly improved the capability of executing multi-modal sensor fusion, improving the robustness of systems, particularly in visually impaired or GPS-denied states. Nevertheless, the difficulty and computational requirements of DL techniques raise issues associated with safety, interpretability, and real-world deployment [11]. To solve these problems, continuous research strives to balance higher performance with effective method design, ensuring that UAVs can operate effectively and safely in real-time applications [12].

Obstacle detection is a basic perception task in autonomous UAV systems that precedes path planning by providing real-time information about the surrounding obstacles. The proposed architecture is designed to accurately identify obstacles using multi-sensor data, thereby supporting safe navigation and facilitating subsequent path planning decisions. Accordingly, the study focuses on developing an explainable obstacle detection framework that enhances environmental perception for UAM applications.

This study presents an innovative explainable deep learning-based UAV path planning approach (XDL-UAVODF) that utilizes multi-sensor data for efficient navigation in urban air mobility systems. The proposed model intends to develop a UAV-based path planning framework for safe and effective navigation in a dynamic environment. Moreover, dependable UAV navigation in practical situations remains challenging. However, reliable UAV navigation in real-world scenarios remains challenging because of difficult environmental factors, multi-dimensional sensor data, and uncertainty in obstacle placement. These tasks need effective feature extraction, capable decision-making, and explainable learning mechanisms. The proposed XDL-UAVODF model follows a comprehensive pipeline that integrates preprocessing, feature selection, dynamic graph-based classification, parameter selection, and model interpretability to improve the performance of the model. The experimental analysis of the proposed XDL-UAVODF methodology takes place utilizing a benchmark dataset, and the outcomes are reported in terms of various measures. The core contributions of this work are outlined below:

- Design a hybrid principal component analysis (PCA) and least absolute shrinkage and selection operator (LASSO) for selecting the most relevant features and, by eliminating less significant features, improve model efficiency.

- Employ a dynamic sparse graph convolutional recurrent network (DSGCGRN) to model spatial-temporal relationships in multi-sensor data and capture dynamic dependencies between features while reducing computational complexity through sparse graph representations.
- Present the AdaGrad optimizer for the process of tuning parameters, which helps to achieve improved performance with limited computational complexity.
- Validate the performance of the XDL-UAVODF approach on the UAV Autonomous Navigation Dataset and evaluate the outcomes under several measures.

2. Literature review

This section briefly reviews prior related works on UAV path planning using multi-sensor data. Liu et al. [13] proposed a multi-phase optimizer structure that combines high-level path planning, obstacle avoidance, and task allocation. A weighted clustering approach has been employed for effective patrol point allocation, assuring a balanced UAV burden. The proposed method is an ant colony optimization (IACO) method for high-level path planning, integrating dynamic pheromone updates and a 2-opt local search approach for refining the paths and enhancing optimization. Weng et al. [14] presented an air traffic management structure that combines collision avoidance and route guidance. The collision avoidance model creates a collision-free aircraft trajectory among the waypoints within 3D space. The route guidance module optimally distributes aircraft through both temporal and spatial dimensions to regulate the paths by enabling larger-scale applications that build a quick, approximate approach for global path planning and accept the velocity obstacle method for distributing collision avoidance. Kim et al. [15] introduced a DL structure that depends on an long short-term memory (LSTM) module, which considers shorter flight dynamics and longer-range dependency in trajectory information. Examination of the attention weights distributed shows that temporal segments most influence the method's outcome, improving interpretability and directing upcoming refinements.

Liu et al. [16] suggested a unified structure that combines infrastructure readiness valuation with daytime running lights (DRL) driven UAV path planning. By utilizing a data-based model integrating clustering examination and in situ measures for estimating the citywide distribution of surveillance quality, the proposed model is an infrastructure-aware path planning method that depends on a deep Q-network (DQN) with a convolutional structure, allowing UAVs to learn effective trajectories while evading surveillance blind regions. Veiga-Piñeiro et al. [17] introduced a computational fluid dynamics (CFD)-based structure that combines a cutting-edge training (CAE) with a deep neural network (DNN) for fast prediction of urban settings and the application of UAV trajectory planning. The CAE reduces the horizontal field of flow into a lower-dimensional hidden space, offering an effective representation of intricate patterns. Deniz and Wang [18] presented a deep multi-agent RL structure specifically adapted to the challenges of eVTOL navigation in 3D space, using a decentralized performance method and centralized learning, leveraging a shared neural network throughout each agent in the system. This model handles larger-scale, high-density eVTOL traffic, ensuring safe separation and conflict resolution at connections and combining points.

Isik et al. [19] presented an innovative machine learning (ML)-driven global navigation satellite system (GNSS) integrity monitoring structure, which integrates environment detection for creating environment-specific error methods. The proposed method leverages the probabilistically predictive abilities of the N grin boost (NGB) methods and establishes higher outcomes of approximating protective levels related to the conventional approach. In [20], an approach for planning UAM route networks was proposed. The planning procedure has been separated into dual phases: optimization and construction. Systems for building UAM route networks that depend on flight routes and global optimizer approaches relying on node movement were presented in all phases. Qin et al. [21] introduced an unsupervised image stitching model utilizing generative adversarial networks (GANs), feature frequency awareness network (FFAN), convolutional block attention module (CBAM), and transformer-based deep homography estimation (TDHE). These models improve image quality, learn hierarchical multi-scale features, and enhance image alignment performance. Qin and Ran [22] presented an unsupervised image stitching method based on YOLOv8, attention mechanism, pooling pyramid module (PPM), deep homography networks (DHN), and adaptive reconstruction. These algorithms enhance feature extraction, assess image transformations, and improve stitching quality by decreasing visual artifacts and alignment errors.

Ngcukayitobi [23] proposed a model with a phased strategic roadmap, which outlines the transition from trials to fully autonomous, AI-based aerial mobility networks. It also highlights the demand for ethical co-design practices, real-world validation environments, and standardized testbeds to ensure social acceptance, compliance, and trust. Ultimately, it underscores the need for multidisciplinary collaboration over AI, urban policy, aerospace engineering, and ethics to realize an intelligent and sustainable UAM future. Song et al. [24] designed a resilient trajectory tracking controller, which ensures that all signals of the closed-loop system are semi-globally uniformly bounded, satisfying the pre-set constraints, even if the anticipated actuator faults occur. Finally, the superiority and feasibility of the designed control method are clarified by simulation results. Table 1 provides the literature review of existing studies on UAV path planning using multi-sensor data.

Table 1. Overview of existing related works.

References	Research aim	Models	Advantages	Disadvantages
Liu et al. [13]	To create collision-free, energy-efficient, and time-optimized paths for urban patrol applications.	Enhanced ant colony optimization	Incorporate task allocation, global planning, and obstacle evasion into a unified framework for improved coordination.	Increased computational complexity due to multi-stage integration of algorithms.
Weng et al. [14]	To combine route guidance and collision avoidance mechanisms for safe and efficient aerial traffic operations.	Route guidance mechanism	Enhances airspace efficiency through optimized traffic coordination.	High computational complexity due to real-time large-scale simulation.
Kim et al. [15]	To improve decision-making and situational awareness using predictive modeling techniques.	DL models	Improves efficiency of UAM operations through predictive analysis.	Requires large amounts of high-quality training data for optimal performance.

Continued on next page

Liu et al. [16]	To integrate infrastructure assessment with strategic optimization for efficient airspace management.	DRL approach	Supports strategic decision-making through intelligent optimization techniques.	System effectiveness may depend on proper parameter tuning and model configuration.
Veiga-Piñeiro et al. [17]	To develop a CFD and DL framework for accurate urban wind flow prediction.	Convolutional autoencoder and deep neural network	Improves UAV safety by accounting for wind-induced disturbances.	High computational cost due to CFD simulations and deep learning integration.
Deniz and Wang [18]	To develop an autonomous conflict resolution framework for UAM systems.	DRL approaches	Supports coordinated decision-making among multiple UAVs using multi-agent learning.	Convergence and stability may be challenging in multi-agent settings.
Isik et al. [19]	To improve navigation safety by detecting and mitigating GNSS errors and signal degradation.	ML techniques	Supports safe and efficient UAV operations in dense urban airspace.	Model generalization may be challenging across different urban scenarios.
Li et al. [20]	To design an optimized and structured airspace network for safe and efficient UAV operations.	Ant colony optimization	Supports large-scale UAM deployment in complex urban environments.	Static network design may be less adaptable to highly dynamic conditions.
Qin et al. [21]	Unsupervised image stitching for robust image alignment below weak textures, challenging light conditions, and significant parallax.	GAN + FFAN + CBAM + TDHE	Enhances image quality, feature extraction, and image alignment performance.	Limited to image stitching; not suitable for UAV path planning.
Qin and Ran [22]	Unsupervised image stitching	YOLOv8 + attention mechanism + deep homography network (DHN) + adaptive reconstruction	Enhances feature extraction and image alignment accuracy and improves stitching quality with reduced artifacts.	Accurate image stitching; limited application to UAV path planning or multi-sensor data fusion

Continued on next page

Ngcukayitobi [23]	AI-driven technologies, deployment methods for autonomous eVTOL drones in UAM.	AI-based UAM architecture, multi-sensor fusion, autonomous navigation, explainable AI	Overview of AI methods, sensor fusion, and UAM integration techniques.	No validation of specific obstacle detection experimentally.
Song et al. [24]	Adaptive control method for autonomous surface vehicles.	Adaptive failure compensation control, composite neural learning.	Enhances fault tolerance, stability and system robustness	Aims at autonomous surface vehicles rather than UAVs.

3. Mathematical model of path planning in the UAM platform

This section discusses the mathematical modeling of the UAM path planning problem formulation, objectives, constraints, and trajectory representation. Consider the urban airspace denoted by a 3D environment

$$E \subset \mathbb{R}^3. \tag{3.1}$$

The starting and end points of the UAM vehicle can be defined as follows:

$$S = (x_s, y_s, z_s), \tag{3.2}$$

$$G = \left(x_g, y_g, z_g\right), \tag{3.3}$$

where x, y, and z denote longitude, latitude, and altitude levels, respectively.

The objective of the UAM path planning is to determine the optimum path without any obstacles, which can be represented as follows:

$$P = \{p_1, p_2, \dots, p_n\} \tag{3.4}$$

such that

$$p_1 = S,\ p_n = G. \tag{3.5}$$

The UAM vehicle path can be denoted by a series of waypoints, as given below:

$$P = \{(x_i, y_i, z_i)\}_{i=1}^{n}. \tag{3.6}$$

The total path length can be denoted as follows:

$$L(P) = \sum_{i=1}^{n-1} \sqrt{(x_{i+1} - x_i)^2 + (y_{i+1} - y_i)^2 + (z_{i+1} - z_i)^2}. \tag{3.7}$$

The aim is the minimization of the weighted cost function, as defined below:

$$J(P) = w_1 C_{dist} + w_2 C_{energy} + w_3 C_{risk}, \tag{3.8}$$

where C_{dist}, C_{energy}, and C_{risk} indicate distance cost, energy utilization, and safety risks of nearby obstacles, respectively. The constraints of obstacle avoidance in the UAM path planning are represented below. Consider the obstacle area to be

$$O = \{o_1, o_2, \dots, o_k\}. \tag{3.9}$$

Every obstacle can be denoted by a 3D region. The constraint is

$$P \cap O = \emptyset, \tag{3.10}$$

indicating that the planned path should not meet any obstacles.

4. Proposed methodology

This study follows a systematic approach for effective UAV path planning using multi-sensor data in urban air mobility environments. Figure 1 illustrates the overall structure of the research framework adopted in this study. The proposed framework comprises five stages, including data preprocessing, feature selection, deep learning-based path planning, optimization, and explainability analysis. The proposed model involves various stages, as represented in Figure 1.

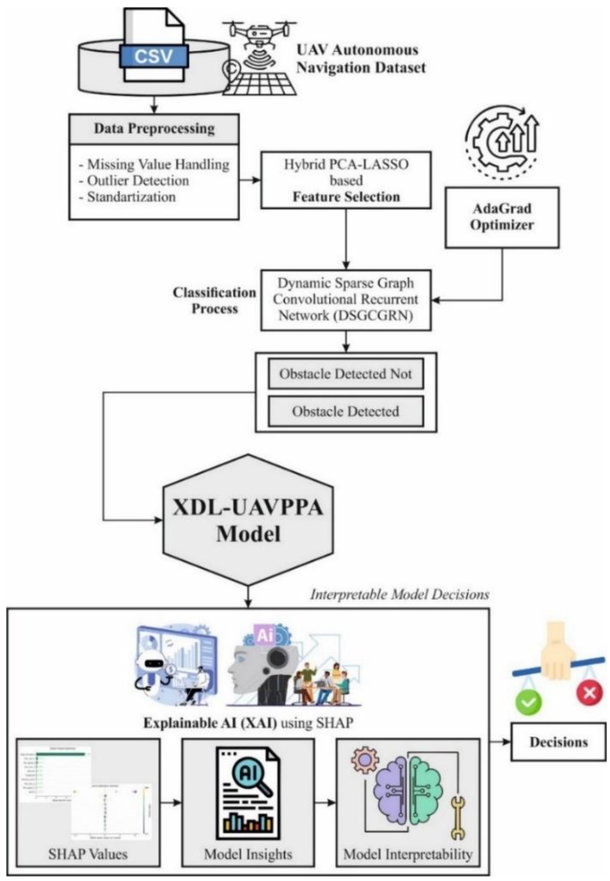

Figure 1. Overall structure of the research methodology.

Data preprocessing: In the initial stage, data preprocessing is used to improve dataset quality and consistency by handling missing values, removing outliers utilizing the interquartile range (IQR) model, and applying standardization to normalize the data for effective model training.

Hybrid feature selection: Once the preprocessing is completed, the hybrid PCA and LASSO technique is used for effective feature selection and reduced dimensionality. It facilitates identifying the most relevant features while eliminating redundant and less important data.

Dynamic graph-based classification: Following that, the DSGCGRN is a deep learning model designed to capture complex spatial-temporal relationships in data. It utilizes sparse graph structures and recurrent mechanisms to efficiently model dynamic dependencies while reducing computational complexity.

Parameter tuning: AdaGrad is used to adaptively adjust the learning rate for each parameter during model training, which helps to improve convergence efficiency and enhances overall model performance.

Model interpretability: SHapley Additive exPlanations (SHAP) is applied for model interpretability and explainability, as it quantifies the contribution of every feature to the prediction model, thereby providing transparent insights into the process of decision-making.

4.1. Preprocessing pipeline

The proposed model starts with data preprocessing, including missing value handling, IQR, and standardization to ensure the input data.

Missing value handling: The databases can comprise missing values due to system interruptions, transmission errors, incomplete recordings, or sensor faults [25]. By handling missing values using forward filling, missing data is filled with the latest accessible observation. Mathematically, let x_t signify the value at time step t, x_t' denotes the imputed value described as

$$x_t' = x_{t-1}, \text{ if } x_t \text{ is missing.}$$

In early steps without prior observation, missing data are initialized using the mean of the accessible data. This preserves data continuity and assures consistency during training and subsequent data preprocessing.

Outlier detection: This is a statistical approach employed for detecting outliers and measuring data variability [26]. The IQR calculates the dispersion of the central 50% of the data, and values outside the upper and lower limits are regarded as potential outliers. It is a strong argument against the maximum value. This method is applied in data preprocessing to enhance data quality and consistency.

Standardization: This is also called z-score normalization. It is an essential preprocessing stage, especially when features have various units and differing numerical ranges. In the absence of scaling, features with higher magnitudes can dominate the learning process. This transforms features to have a mean of 0 and a standard deviation of 1, assuring that every feature contributes equally to the learning process and enhancing the stability and convergence of optimal models.

4.2. Hybrid feature selection frameworks

The hybrid PCA-LASSO method is integrated into the UAV path planning framework to reduce data dimensionality while selecting the most relevant features from multi-sensor inputs. PCA normalizes the information, calculates the covariance matrix, and performs eigenvalue decomposition to classify the principal components that represent the most significant differences in the data [27]. LASSO regression further refines this representation by decreasing the coefficients of less significant features to 0. This incorporation enhances computational efficacy and method precision by maintaining only the most informative features.

PCA: This is a statistical model that converts correlated components into uncorrelated elements, taking the maximal difference in the data. For the database $X\in \mathbb{R}^{n\times p}$ with n monitoring and p features, PCA calculates the following:

- Standardization:

$$X' = \frac{X-\mu}{\sigma}.$$

Let μ denote the feature-wise mean, and σ signify the feature-wise SD.

- Covariance matrix computation:

$$\Sigma = \frac{1}{n-1}(X')^T X'.$$

- Eigenvalue decomposition:

$$\Sigma = V\Lambda V^T.$$

Here, V covers the eigenvectors, and Λ represents the diagonal eigenvalue matrix.

- Projection onto principal components:

$$X_{PCA} = X'V_k.$$

Here, V_k represent the top k eigenvectors, which describe the most variance.

LASSO: The regression model improves model explainability by applying regularization and variable selection. With a dataset $X\in \mathbb{R}^{m\times q}$, $y \in \mathbb{R}^m$ is the response vector, and LASSO addresses the optimum issue:

$$\hat{\gamma} = \arg\min_{\gamma}\left\{\frac{1}{2m}\sum_{i=1}^{m}(y_i - \sum_{k=1}^{q} X_{ik}\,\gamma_k)^2 + \lambda\sum_{k=1}^{q}|\gamma_k|\right\}.$$

In the formula, $\hat{\gamma}$ denotes the optimized regression coefficient vector, X_{ik} presents the k-th feature of the i-th sample, and y_i is the expected output. The first term minimizes the mean squared error between actual and predicted values, whereas the second L1 regularization term $\lambda\sum|\gamma_k|$ achieves sparsity by removing irrelevant coefficients toward zero, thus enhancing feature selection performance and model simplification.

In this formula, $\lambda \geq 0$ controls the shrinking coefficients, removing insignificant features and penalty strength. A hybrid PCA and LASSO for feature selection utilizes the following phases:

PCA transformation:

- Normalize the data and calculate principal components.
- Select the top k components that explain the highest variance.

PCA and LASSO are combined to use their supportive capabilities in feature selection. The PCA algorithm first reduces the irrelevant features and changes the raw data into a compact feature representation, whereas the LASSO method recognizes the important features by removing unimportant variables. By combining PCA with LASSO, this method efficiently minimizes dimensionality while retaining vital predictive information, thereby improving model effectiveness and explainability.

4.3. Dynamic sparse graph-based path planning

The DSGCGRN is designed to examine intricate patterns in data and enhance decision-making performance. In real-time dynamic models, the relationship among entities is time-dependent, leading to the development of spatial dependency. To address these intricate relationships, graph convolutional networks (GCNs) are employed to capture structural relations within graph-driven information [28]. At the same time, conventional GCNs based on static graph models restrict their capability of representing time-varying correlations. Dynamic GCNs overcome this limitation by adapting the updating adjacency matrices, allowing efficient learning of changing spatial relations in dynamic situations.

The DSGCGRN comprises numerous layers of DSGCN-GRU models, with each gated recurrent unit (GRU) integrating dual blocks of DSGCN and a single block of graph attention. By incorporating the capabilities of DSGCN and GRU, the method is capable of capturing both spatial and temporal correlations. The DSGCN mechanism updates the adjacency matrix based on the evolving data, thus accounting for the shifting spatial correlations within the network over time. The sparse graph learning model supports the technique for identifying explicit relationships, efficiently restricting the spatial yielding region to maintain the distinct features of specific nodes. Meanwhile, the GRU elements manage the storage and processing of time-series data. Figure 2 depicts the architecture of the DSGCN model.

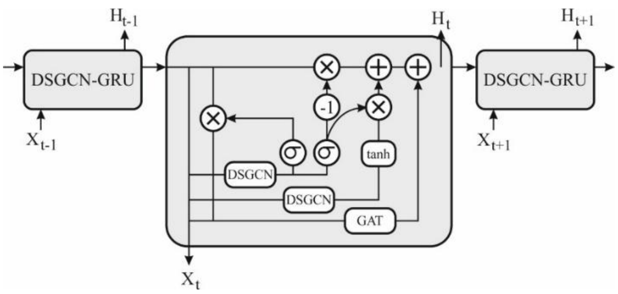

Figure 2. Architecture of the DSGCN model.

Primarily, the model generates an adaptive node embedded to compute the matrix of adjacency $A \in R^{N\times N}$. Then, it utilizes a sparsification model to A, preventing only the higher resemblance connections among all nodes and adjacent nodes. The resultant matrix has been standardized employing the softmax function by gaining an adaptive sparse matrix of adjacency $S_A \in R^{N\times N}$, $A = ReLU(EE^T)$.

$$S_A = softmax\left(ReLU\big(sparsify(A;k)\big)\right).$$

Let $E \in R^{N\times d}$ denote the adaptive node embedding matrix. Here, d implies the dimensionality of node embedding. The operation $sparsify(*)$ implies the function of sparsification, and k signifies the rate of sparsity. To facilitate the approach for learning high-order neighboring data in graph information, we employ Chebyshev polynomials to estimate the kernel of graph convolution.

This enables us to effectively model the complex interactions among the nodes, as well as the different neighbors and the wider global structure, without major growth in computational difficulty.

4.4. AdaGrad optimization

AdaGrad is employed to adaptively adjust the learning rate during model training, improving convergence and enhancing optimization efficiency and stability in complex learning tasks. AdaGrad is a gradient-driven optimizer model that separately adapts the learning rate for all parameters [29]. The main idea of the model is to apply a lower learning rate for parameters connected with recurrent aspects and a higher learning rate for parameters related to rare features. The AdaGrad optimizer model is calculated as follows:

$$\theta_{t+1,i} = \theta_{t,i} - \eta \frac{1}{\sqrt{G_{t,ii}+\varepsilon}} g_{t,i}.$$

In this formula, $g_{t,i}$ represents the loss function gradient for parameters $\theta_{t,i}$ at time step t. This is a smooth term designed to evade division by zero. The diagonal matrix represented by $G_{t,ii}$ signifies the number of gradient squares for parameter $\theta_{t,i}$ at time step t. The approach removes the essential for adapting the learning rate. Hence, the learning rate can shrink, and the convergence can reduce due to accumulating the gradient squares in the denominator.

Table 2 indicates the parameter settings of the proposed model. The hyperparameters are configured to optimize the performance of the proposed model during training. The learning rate (0.001) regulates the step size for weight updates, ensuring stable convergence. A batch size of 32 balances training efficiency and computational stability. Three graph convolution layers and 64 hidden units enable effective feature learning and spatial-temporal representation. A dropout rate of 0.3 is applied to reduce overfitting and improve model generalization.

Table 2. Parameter setting.

Hyperparameter	Description	Optimized value
Learning rate	Step size used by the optimizer for updating weights	0.001
Batch size	Number of samples processed in one training iteration	32
Number of graph convolution layers	Depth of the graph convolution network	3
Hidden units	Number of neurons in recurrent layers	64
Dropout rate	Regularization to prevent overfitting	0.3

4.5. Model interpretability

SHAP is applied to explain feature contributions and improve the transparency of the DL approach. SHAP values offer a single measurement of feature significance that depends on cooperative game theory. SHAP values were calculated for all attributes x_i within the input data [30]. These values signify the contributions of all attributes to the prediction. For a provided method f and a sample x, ϕ_i denotes the SHAP value for feature i, expressed as

$$\phi_i = \sum_{S \subseteq N\setminus j} \frac{|S|!(|N|-|S|-1)!}{|N|!}[f(S \cup i) - f(S)].$$

Here, N denotes the collection of each feature, S denotes the subdivision of features, $f(S)$ implies the prediction of the method for the subdivision S, and $f(S \cup i)$ implies the prediction of the method involving feature i. The reliability of SHAP values arises from their respect for theoretical properties, including symmetry and additivity, which offer a basis of principles for feature significance in a model-independent way. Although parameter weights signify relations learned within the method, they frequently reflect only the internal state of networks and do not contain an interpretable or direct map to the input feature importance. However, SHAP values measure all features as predictive of the method by determining their marginal impact on the outcome, thus providing a direct explanation of feature significance.

The rationale for employing hybrid PCA-LASSO to obtain an informative and compact feature set is the use of the AdaGrad optimizer during model training and the dynamic sparse graph convolutional recurrent network (DSGCRN) for jointly capturing temporal dependencies and spatial relationships in UAV navigation. Additionally, the integration of the SHAP-based explainability module has been detailed to demonstrate how feature-level contributions are explained to support autonomous navigation decisions and transparent obstacle detection, which shows greater emphasis on the proposed integration method and the design choices that distinguish the proposed framework from traditional UAV navigation pipelines.

5. Performance validation

In this section, the performance assessment of the XDL-UAVODF approach is evaluated under the UAV Autonomous Navigation dataset [31]. The UAV Autonomous Navigation and Obstacle Avoidance Sensor Dataset is intended to support research on DL-based autonomous flight and obstacle detection. This dataset combines multi-sensor data, comprising GPS, LiDAR, IMU, and UAV telemetry, to enable obstacle avoidance and real-time path planning. It offers extensive environmental data and precise navigation in complex and dynamic scenarios. The dataset consists of 5000 samples with dual classes, as depicted in Table 3.

Table 3. Dataset details.

Detection	Samples
Obstacle Detected Not	4764
Obstacle Detected	236
Total	**5000**

Figure 3 demonstrates the correlation matrix of the XDL-UAVODF approach. This matrix shows the relationship among diverse features in the dataset. The values range from -1 to +1, representing negative, positive, or no correlation. Most features exhibit very low correlation, meaning there is minimal redundancy among them. This indicates that the chosen features are largely independent.

Figure 4 depicts the distribution of lidar distance for dual classes: obstacle detected (1) and not detected (0). When no obstacle is identified (0), the lidar distances are extensively spread with a higher median value. The data for class 0 ranges nearly from low to very high distances, indicating greater variability. When an obstacle is detected (1), the lidar distances are much smaller and tightly clustered. This clearly illustrates that shorter lidar distances are associated with obstacle detection.

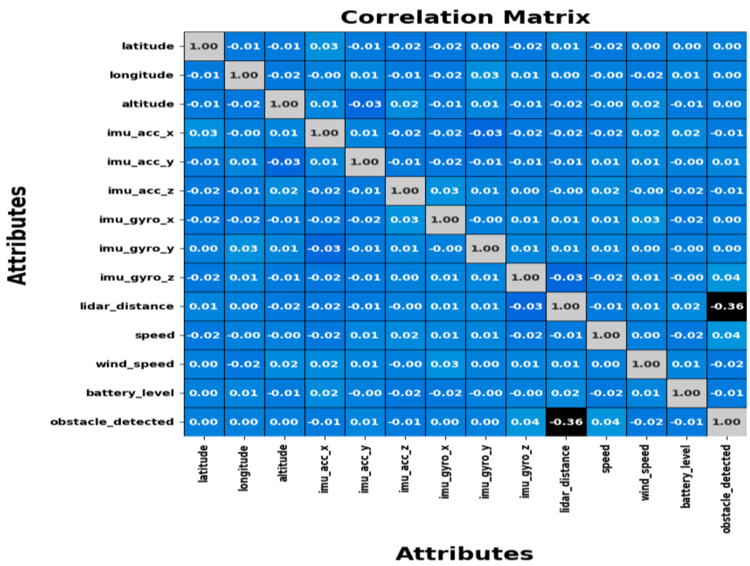

Figure 3. Correlation matrix of the XDL-UAVODF method.

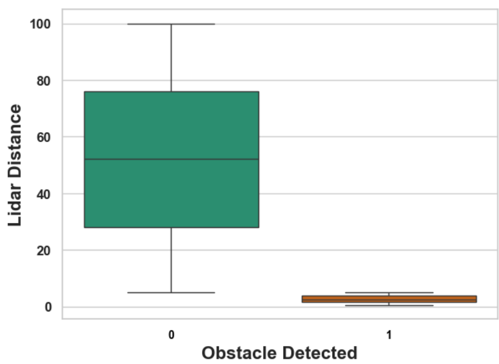

Figure 4. Obstacle detection vs. lidar distance.

Figure 5 depicts the relationship between battery level and speed, with data points densely spread throughout the ranges. Battery levels vary from 20 to 100, while speed ranges from 5 to 30. The distribution appears random, representing no clear correlation between battery level and speed in the dataset.

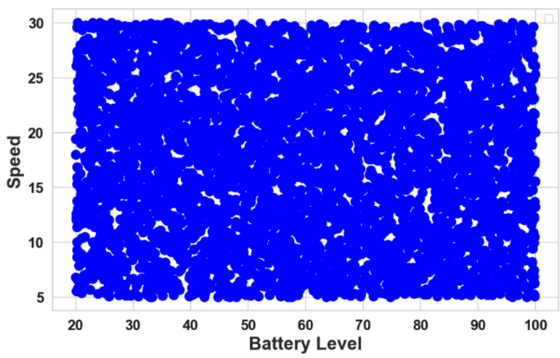

Figure 5. Speed vs. battery level.

Figure 6 presents the confusion matrices generated by the XDL-UAVODF technique. The results demonstrate that the XDL-UAVODF method accurately identifies and classifies all classes with high precision.

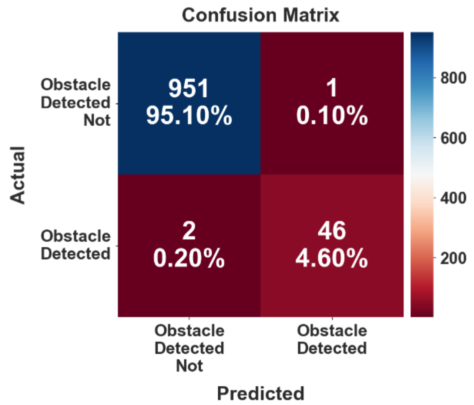

Figure 6. Confusion matrix of the XDL-UAVODF approach.

Table 4 shows the obstacle detection performance of the proposed framework using an 80:20 training/testing split. The obtained outcomes indicate that the proposed model efficiently classifies non-obstacle and obstacle samples with high reliability. For the 80% training data, the XDL-UAVODF framework achieves average values of 96.24% accuracy, 94.02% precision, 96.24% recall, 95.10% F-score, 96.24% area under the curve (AUC)-score, 90.23% Matthews correlation coefficient (MCC), and 96.24% balanced accuracy. Meanwhile, for the 20% testing data, the proposed framework attains average values of 97.86% accuracy, 98.83% precision, 97.86% recall, 98.34% F-score, 97.86% AUC-score, 96.69% MCC, and 97.86% balanced accuracy. These results show the effectiveness of the proposed model in maintaining consistent obstacle detection performance over both training and testing datasets.

Table 4. Obstacle detection result of the XDL-UAVODF method with an 80:20 training/testing split.

Class labels	**Accuracy**	**Precision**	**Recall**	**F-score**	**AUC-score**	**MCC**	**Balanced accuracy**
TRAP (80%)							
Obstacle Detected Not	99.4	99.66	99.4	99.53	96.24	90.23	
Obstacle Detected	93.09	88.38	93.09	90.67	96.24	90.23	96.24
Average	96.24	94.02	96.24	95.1	96.24	90.23	
TESP (20%)							
Obstacle Detected Not	99.89	99.79	99.89	99.84	97.86	96.69	
Obstacle Detected	95.83	97.87	95.83	96.84	97.86	96.69	97.86
Average	97.86	98.83	97.86	98.34	97.86	96.69	

Figure 7 denotes the training (TRAING) and validation (VALIDN) accuracy curves of the XDL-UAVODF approach on an 80:20 training/testing split over 50 epochs. The TRAING accuracy is constantly increasing, depicting effective learning and proper convergence of the approach. The

VALIDN accuracy nearly follows the training curve with a smaller gap, representing lower overfitting and improved generalization performance.

Figure 8 demonstrates the TRAING and VALIDN loss curves of the XDL-UAVODF system with an 80:20 training/testing split over 50 epochs. Both losses fall significantly in the initial epochs and then progressively stabilize, indicating effective convergence and learning. The smaller gap between TRAING and VALIDN loss validates improved generalization and lower overfitting.

Figure 9 exhibits the confusion matrices created by the XDL-UAVODF method. The results demonstrate that the XDL-UAVODF approach accurately detects and identifies each class with higher precision.

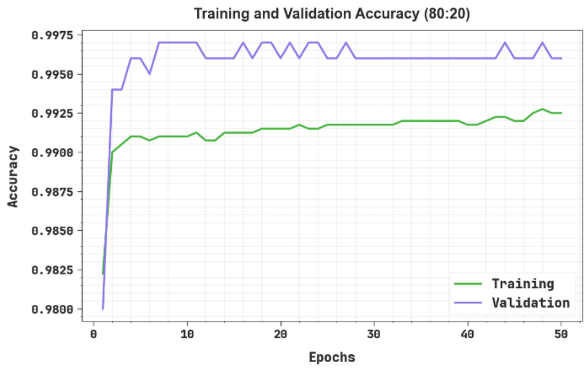

Figure 7. Accuracy curve of the XDL-UAVODF approach with an 80:20 training/testing split.

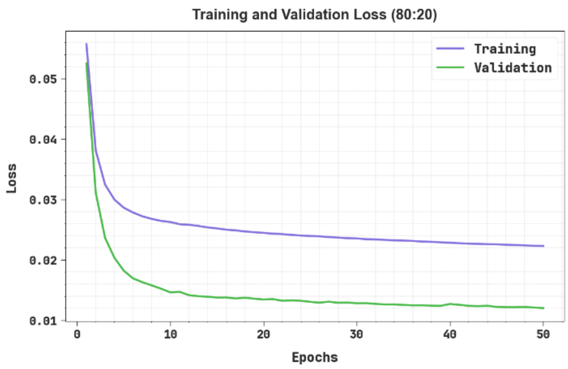

Figure 8. Loss curve of the XDL-UAVODF technique with an 80:20 training/testing split.

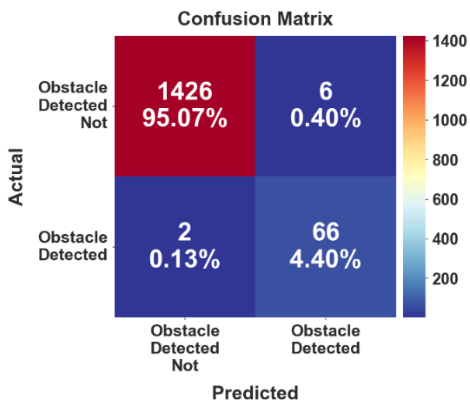

Figure 9. Confusion matrix of the XDL-UAVODF approach.

Table 5 illustrates the obstacle detection performance of the proposed XDL-UAVODF architecture using a 70:30 training/testing split. The obtained results show that the proposed model effectively differentiates between non-obstacle and obstacle classes. For the 70% training (TRAP) data, the proposed framework achieves average values of 98.14% accuracy, 93.28% precision, 98.14% recall, 95.56% F-score, 98.14% AUC-score, 91.28% MCC, and 98.14% balanced accuracy. Similarly, for the 30% testing (TESP) data, the proposed framework attains average values of 98.32% accuracy, 95.76% precision, 98.32% recall, 97.00% F-score, 98.32% AUC-score, 94.05% MCC, and 98.32% balanced accuracy. These results confirm the robustness of the proposed model in achieving reliable obstacle classification with persistent performance over both training and testing datasets.

Table 5. Obstacle detection result of the XDL-UAVODF method with a 70:30 testing split.

Class labels	**Accuracy**	**Precision**	**Recall**	**F-score**	**AUC-score**	**MCC**	**Balanced accuracy**
TRAP (70%)							
Obstacle Detected							
Not	99.25	99.85	99.25	99.55	98.14	91.28	98.14
Obstacle Detected	97.02	86.7	97.02	91.57	98.14	91.28	
Average	98.14	93.28	98.14	95.56	98.14	91.28	
TESP (30%)							
Obstacle Detected							
Not	99.58	99.86	99.58	99.72	98.32	94.05	98.32
Obstacle Detected	97.06	91.67	97.06	94.29	98.32	94.05	
Average	98.32	95.76	98.32	97	98.32	94.05	

Figure 10 shows the TRAING and VALIDN accuracy curves of the XDL-UAVODF technique on a 70:30 training/testing split over 50 epochs. The TRAING accuracy steadily increases, signifying effective learning and appropriate convergence of the method. The VALIDN accuracy nearly follows the training curve with a smaller gap, signifying minimal overfitting and better generalization outcomes.

Figure 11 exemplifies the TRAING and VALIDN loss curves of the XDL-UAVODF method with a 70:30 training/testing split through 50 epochs. Both losses decline rapidly in the early epochs and then gradually stabilize, indicating effective convergence and learning. The lower gap between the TRAING and VALIDN loss validates better generalization and reduced overfitting.

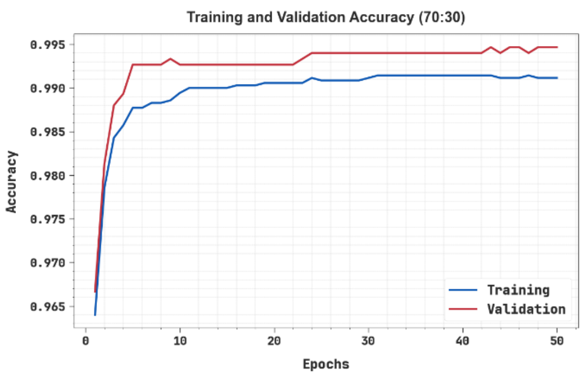

Figure 10. Accuracy curve of the XDL-UAVODF approach with a 70:30 training/testing split.

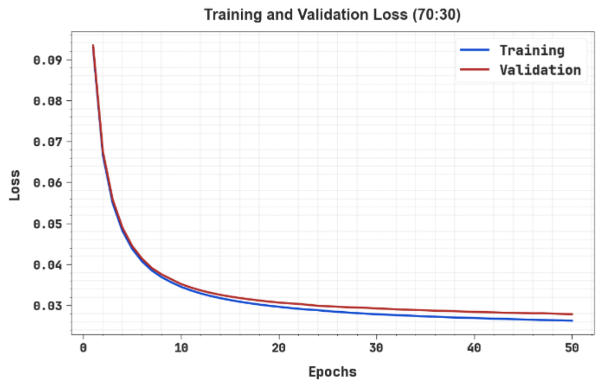

Figure 11. Loss curve of the XDL-UAVODF technique with a 70:30 training/testing split.

The comparative examination of the XDL-UAVODF techniques with other existing systems is shown in Table 6 [32]. The experimental outcomes indicate that the proposed methodology has enhanced performance. It is designed as an application-level comparison with representative DL approaches used in UAV-based navigation and detection studies. The selected methods, including YOLOv3, YOLOv5, RetinaNet, and MobileNet, primarily use image-based inputs, whereas the proposed framework works on tabular sensor fusion data. Hence, it provides a broader performance perspective in demonstrating the effectiveness of the proposed framework for UAV autonomous navigation.

Table 6. Comparison study of the XDL-UAVODF approach with existing models.

Methods	Accuracy	Error rate (%)	Precision	Recall	F-score
FCN	87.95	12.05	88.98	90.51	86.78
ConvPoint	92.10	7.90	93.83	88.91	92.33
MobileNet	72.20	27.80	85.16	87.28	91.80
YOLOv3	92.00	8.00	88.57	85.94	91.97
RetinaNet	88.00	12.00	94.06	86.11	85.92
YOLOv5	84.00	16.00	89.16	89.29	87.21
BS-CYOLOv5	95.00	5.00	90.45	90.39	91.22
XDL-UAVODF	98.32	1.68	95.76	98.32	97.00

The results indicate that the logistic regression (LR), bagging, and Naïve Bayes (NB) models showed worse performance. Meanwhile, the support vector machine (SVM), voting, and K-nearest neighbor (KNN) models presented closer results. Furthermore, the XDL-UAVODF model reported improved performance, with maximum farming community network (FCN), MobileNet, RetinaNet, and YOLOv5n models having the least outcomes, while ConvPoint and YOLOv3 achieved slightly greater performance. Moreover, the BS-CYOLOv5 method performed well and had closer results, with an accuracy of 95.00%, precision of 90.45%, recall of 90.39%, and F-score of 91.22%. Lastly, the proposed XDL-UAVODF model achieved superior performance with an accuracy of 98.32%, precision of 95.76%, recall of 98.32%, and F-score of 97.00% as shown in Figure 12.

Figure 13 presents the comparative results of the XDL-UAVODF technique in terms of error rate. The performance indicates that the proposed XDL-UAVODF technique achieves a lower error rate of

1.68%, while the FCN, ConvPoint, MobileNet, YOLOv3, RetinaNet, YOLOv5, and BS-CYOLOv5 models reached higher error rates of 12.05%, 7.90%, 27.80%, 8.00%, 12.00%, 16.00%, and 5.00%, respectively.

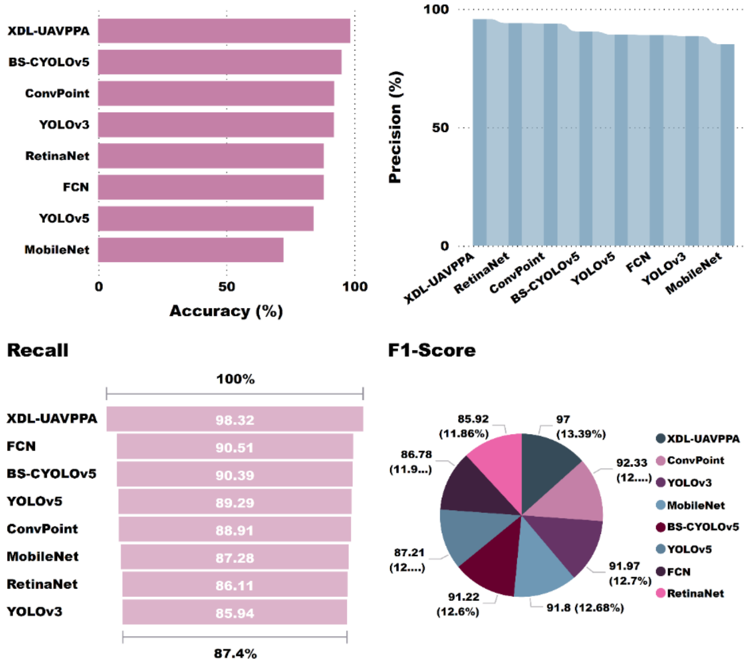

Figure 12. Comparative outcomes of the XDL-UAVODF method with various measures.

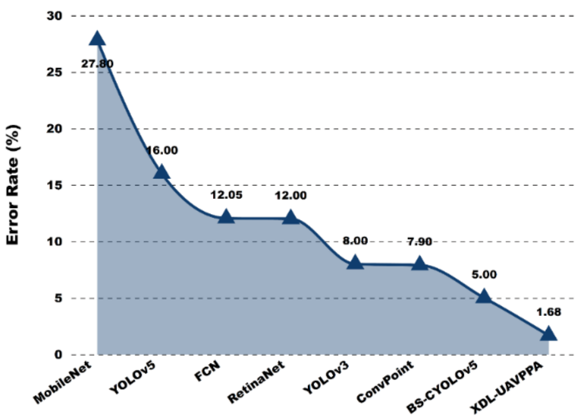

Figure 13. Error rate of the XDL-UAVODF approach with other models.

Table 7 presents the ablation analysis of the proposed framework to assess the contribution of individual components. The baseline DSGCGRN achieves 91.84% accuracy, while the integration of AdaGrad, PCA, and LASSO progressively enhances the classification performance. The combined PCA+LASSO+DSGCGRN model obtains 97.04% accuracy, whereas the complete XDL-UAVODF framework (PCA+LASSO+DSGCGRN+AdaGrad) achieves the highest performance with 98.32% accuracy, 95.76% precision, 98.32% recall, 97.00% F1-score, 98.32% AUC-score, and 94.05% MCC. These results validate the efficiency of each component and show the advantage of the proposed architecture.

Table 7. Ablation study of the XDL-UAVODF approach.

Methods	Accuracy	Precision	Recall	F1-score	AUC-score	MCC
DSGCGRN	91.84	89.76	91.84	90.68	92.05	84.37
DSGCGRN+AdaGrad	92.76	90.91	92.76	91.82	92.98	86.12
PCA+DSGCGRN	94.28	92.63	94.28	93.44	94.51	88.76
LASSO+DSGCGRN	95.13	93.71	95.13	94.41	95.32	90.31
PCA+LASSO	93.46	91.84	93.46	92.64	93.72	87.45
PCA+LASSO+DSGCGRN	97.04	94.66	97.04	95.84	97.18	92.68
XDL-UAVODF (PCA+LASSO+DSGCGRN +AdaGrad)	**98.32**	**95.76**	**98.32**	**97.00**	**98.32**	**94.05**

Table 8 presents the K-fold cross-validation results of the proposed framework to evaluate its generalization and consistency capability. The model attains stable performance across all folds, with mean values of 96.09% accuracy, 92.96% precision, 96.51% recall, 94.71% F1-score, 96.84% AUC-score, and 91.37% MCC. The low standard deviation values indicate that the consistent classification performance over different data splits shows the reliability and robustness of the proposed architecture for UAV obstacle detection.

Table 8. K-fold cross-validation results of the XDL-UAVODF framework.

K-fold	Accuracy	Precision	Recall	F1-score	AUC-score	MCC
k-1	95.82	92.61	96.18	94.36	96.54	90.72
k-2	96.47	93.38	96.81	95.06	97.03	91.86
k-3	94.91	91.12	95.44	93.23	95.88	89.54
k-4	96.82	93.95	97.14	95.52	97.31	92.48
k-5	95.36	92.04	95.83	93.90	96.37	90.31
k-6	96.71	93.76	97.02	95.36	97.25	92.16
k-7	**97.14**	**94.32**	**97.71**	**96.10**	**97.84**	**93.11**
k-8	95.58	92.47	95.94	94.17	96.48	90.65
k-9	96.94	94.08	97.36	95.69	97.56	92.74
k-10	95.19	91.88	95.62	93.71	96.11	90.08
Mean±SD	**96.09±0.76**	**92.96±0.98**	**96.51±0.76**	**94.71±0.90**	**96.84±0.64**	**91.37±1.16**

Figure 14 shows the global and local feature importance for the method utilizing SHAP values. The global feature significance shows that lidar distance has a higher effect on the technique, greatly exceeding other features. The other features, such as imu_acc_x, imu_gyro_z, and altitude, contribute less but still positively influence the predictions. However, local explanation shows how separate feature values impact the output of the model through various samples, with certain points displaying stronger negative or positive impacts.

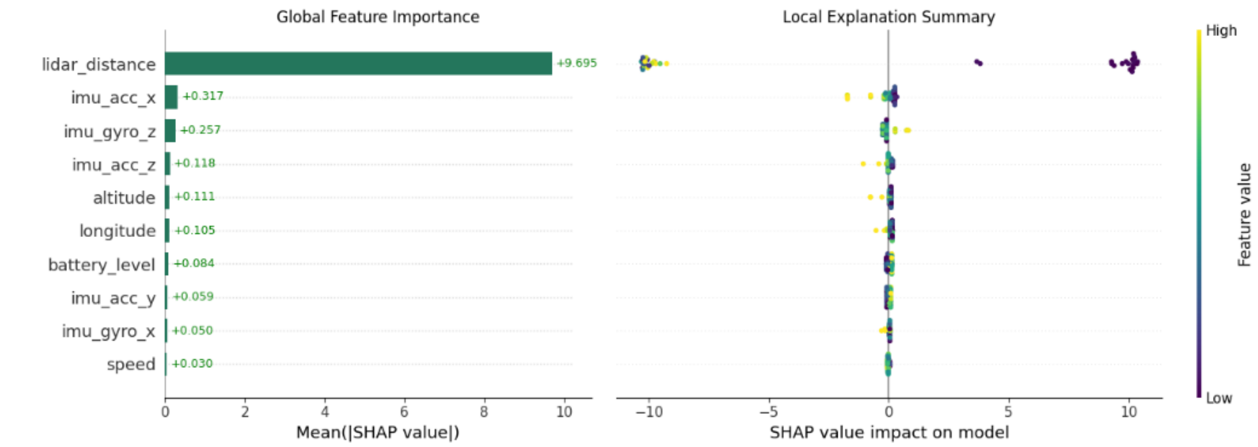

Figure 14. SHAP value.

6. Conclusions

This paper presented the XDL-UAVODF utilizing multi-sensor data for UAM path planning. The major goal of this work is to develop a UAV navigation framework for obstacle avoidance and improved trajectory planning in dynamic environments. Toward this objective, data preprocessing is carried out to ensure clean and consistent input data for model training. For feature selection, a hybrid model that incorporates PCA and LASSO is employed to lessen data dimensionality and choose substantial feature subsets. Furthermore, the DSGCGRN is used to examine intricate patterns in the data and enhance decision-making performance. The AdaGrad optimizer is utilized to adaptively update the learning rate during model training to improve convergence. Finally, SHAP is applied to explain feature contributions and improve the transparency of the DL approach. The performance validation analysis of the XDL-UAVODF model is conducted using the UAV Autonomous Navigation Dataset. The experimental results report the supremacy of the XDL-UAVODF methodology with an accuracy of 98.32% under numerous measures. In future work, the proposed method will be comprehensively validated in real-world UAV deployment scenarios to assess its practical feasibility, robustness, and performance under real-time environmental conditions.

Author contributions

S. A. Alzakari and S. Sorour: Conceptualization; S. A. Alzakari, S. Alghamdi and A. O. A. Ismail: Data curation, Formal analysis; S. A. Alzakari, S. Sorour and A. O. A. Ismail, F. F. Alruwaili , S. A. Asklany: Funding support, Investigation, Methodology; F. F. Alruwaili: Project administration, Resources; S. A. Alzakari, S. Sorour, S. Alghamdi, A. O. A. Ismail, N. Almashfi, A. Blfgeh, S. A. Asklany: Discussion, Writing–review and editing, Writing–original draft; F. F. Alruwaili: Software, Supervision, Validation, Visualisation. All authors have read and agreed to the published version of the manuscript.

Use of Generative-AI tools declaration

The authors declare that they have not used Artificial Intelligence (AI) tools in the creation of this article.

Funding

The authors extend their appreciation to the Deanship of Research and Graduate Studies at King Khalid University for funding this work through Large Research Project under grant number RGP2/286/46. This work was supported by the Deanship of Scientific Research, Vice Presidency for Graduate Studies and Scientific Research, King Faisal University, Saudi Arabia, under project Grant KFU264144). Princess Nourah bint Abdulrahman University Researchers Supporting Project number (PNURSP2026R716), Princess Nourah bint Abdulrahman University, Riyadh, Saudi Arabia. The authors extend their appreciation to the Deanship of Scientific Research at Northern Border University, Arar, KSA for funding this research work through the project number "NBU-FPEJ-2026-2932-05". The author would like to thank the Deanship of Scientific Research at Shaqra University for supporting this work.

Conflict of interest

The authors declare that they have no conflicts of interest.

References

1. G. S. Li, J. C. Dai, J. H. Wang, X. Y. Jing, T. Zhao, D. Q. Chen, Graph neural network and dynamic graph reconstruction based adaptive path planning method for unmanned aerial vehicles (UAVs) in three-dimensional environments, *Meas. Sci. Technol.*, **37** (2026), 056304. https://doi.org/10.1088/1361-6501/ae39fb
2. S. J. Yang, J. T. Yuan, Z. P. Zhang, Z. B. Chen, H. C. Zhang, X. H. Cui, Multi-UAV collaborative mission planning method for self-organized sensor data acquisition, *Comput. Mater. Con.*, **81** (2024), 1529–1563. https://doi.org/10.32604/cmc.2024.055402
3. Y. X. Liu, Q. X. Zhou, W. C. Mao, X. L. Li, H. F. Wei, M. Tsukada, Multi-modal trajectory planning for emergency-oriented air-ground collaborative sensing and communication, *IEEE Trans. Cogn. Commun. Netw.*, **11** (2025), 3094–3111. https://doi.org/10.1109/TCCN.2025.3585254
4. Y. L. Zhang, Z. L. Sun, W. H. Peng, Y. Q. Lin, X. T. Li, K. T. Yan, et al., Key technologies for intelligent operation of plant protection UAVs in hilly and mountainous areas: progress, challenges, and prospects, *Agronomy*, **16** (2026), 193. https://doi.org/10.3390/agronomy16020193
5. D. Z. Yuan, Y. X. Zhong, X. P. Zhu, Y. Chen, Y. Jin, X. Z. Du, et al., Trajectory planning for unmanned vehicles on airport apron under aircraft-vehicle-airfield collaboration, *Sensors*, **25** (2025), 71. https://doi.org/10.3390/s25010071
6. C. Y. Yin, C. W. Wang, Z. K. Huang, H. Jiang, J. Chen, X. R. Miao, CiUAV: Scalable device-free indoor UAV localization via multiobjective optimized network using channel state information, *IEEE Int. Things J.*, **13** (2026), 15297–15307. https://doi.org/10.1109/JIOT.2026.3654645
7. Z. Haider, C. J. Sreenan, K. N. Brown, A. O'Mahony, Indoor autonomous multi-UAVs: a review of current research, enabling technologies and open challenges, *IEEE Access*, **13** (2025), 212231–212265. https://doi.org/10.1109/ACCESS.2025.3642189

8. V. P. Modcoicar, T. Baraskar, ML-driven analysis of NavIC-based tracking for route optimization in urban air mobility, In: *Inventive communication and computational technologies,* Cham: Springer, 2025, 315–328. https://doi.org/10.1007/978-3-032-04312-2_26
9. T. Lombaerts, E. Kawamura, K. Kannan, C. A. Ippolito, V. Stepanyan, G. Gorospe, et al., Cross validation of sensor inputs as part of position estimation for urban air mobility, In: *AIAA SCITECH 2026 Forum,* 2026, 2576. https://doi.org/10.2514/6.2026-2576
10. G. Ariante, U. Papa, *Embedded platforms for UAS landing path and obstacle detection II: Navigation support systems for urban air mobility operations*, Cham: Springer, 2024. https://doi.org//10.1007/978-3-031-59754-1
11. V. Donato, G. Giangreco, F. Mattei, C. Conte, G. Rufino, D. Accardo, et al., Error analysis of extensive drone flight data for satellite navigation in urban environment, In: *AIAA SCITECH 2026 Forum*, 2026, 1071. https://doi.org/10.2514/6.2026-1071
12. C. CHERIF, M. MAIZA, A. TALEB-AHMED, A study on autonomous navigation and obstacle avoidance systems for UAVs using deep learning techniques, 2025, submitted for publication. https://doi.org/10.21203/rs.3.rs-7303597/v1
13. G. Liu, Y. Tang, Z. P. Tan, M. W. Fang, A multi-stage optimization strategy for multi-UAV path planning in complex urban 3D environments with obstacle avoidance, *Complex Intell. Syst.*, **12** (2026), 17. https://doi.org/10.1007/s40747-025-02159-2
14. C. Q. Weng, C. Chen, J. J. Tan, T. L. Pan, R. X. Zhong, Real-time traffic simulation and management for large-scale urban air mobility: integrating route guidance and collision avoidance, *Transport. Res. Part C Emerging Technol.*, **183** (2026.), 105477. https://doi.org/10.1016/j.trc.2025.105477
15. J. Kim, H. Yoon, S. Yoon, Y. Kwon, K. Lee, A deep learning-based trajectory and collision prediction framework for safe urban air mobility, *Drones*, **9** (2025), 460. https://doi.org/10.3390/drones9070460
16. Q. Y. Liu, W. Dai, Z. C. Yan, C. J. Tessone, An intelligent path planning system for urban airspace monitoring: from infrastructure assessment to strategic optimization, *Smart Cities*, **8** (2025), 100. https://doi.org/10.3390/smartcities8030100
17. G. Veiga-Piñeiro, E. Aldao-Pensado, E. Martín-Ortega, Hybrid CFD-deep learning approach for urban wind flow predictions and risk-aware UAV path planning, *Drones*, **9** (2025), 791. https://doi.org/10.3390/drones9110791
18. S. Deniz, Z. B. Wang, Autonomous conflict resolution in urban air mobility: a deep multi-agent reinforcement learning approach, In: *AIAA AVIATION FORUM AND ASCEND 2024*, 2024, 4005. https://doi.org/10.2514/6.2024-4005
19. O. K. Isik, I. Petrunin, A. Tsourdos, Machine learning-based environment-aware GNSS integrity monitoring for urban air mobility, *Drones*, **8** (2024), 690. https://doi.org/10.3390/drones8110690
20. J. Li, D. Shen, F. P. Yu, D. Qi, A method for air route network planning of urban air mobility, *Aerospace*, **11** (2024), 584. https://doi.org/10.3390/aerospace11070584
21. A. K. Biswas, M. S. A. Bhuiyan, M. N. H. Mir, A. Rahman, M. F. Mridha, M. R. Islam, A dual output temporal convolutional network with attention architecture for stock price prediction and risk assessment, *IEEE Access*, **13** (2025), 53621–53639.
22. C. B. Qin, X. T. Ran, D. H. Zhang, Unsupervised image stitching based on generative adversarial networks and feature frequency awareness algorithm, *Appl. Soft Comput.*, **183** (2025), 113466. https://doi.org/10.1016/j.asoc.2025.113466

23. M. Ngcukayitobi, Artificial intelligence-driven design and deployment of autonomous eVTOL drones for urban air mobility: a comprehensive review of challenges, technologies, and integration strategies, *CEAS Aeronaut. J.*, 2026. https://doi.org/10.1007/s13272-026-00985-9
24. S. Song, Y. Jiang, X. Song, V. Stojanovic, Composite neural learning-based adaptive actuator failure compensation control for full-state constrained autonomous surface vehicle, *Neural Comput. Appl.*, **37** (2025), 6369–6381. https://doi.org/10.1007/s00521-024-10651-y
25. C. B. Qin, X. T. Ran, Efficient unsupervised image stitching using attention mechanism with deep homography estimation, *Comput. Mater. Contin.*, **79** (2024), 1319–1334. https://doi.org/10.32604/cmc.2024.048850
26. P. K. Dongre, V. Patel, U. Bhoi, N. N. Maltare, An outlier detection framework for air quality index prediction using linear and ensemble models, *Decis. Anal. J.*, **14** *(*2025), 100546. https://doi.org/10.1016/j.dajour.2025.100546
27. P. K. Sahu, T. Fatma, Optimized breast cancer classification using PCA-LASSO feature selection and ensemble learning strategies with Optuna optimization, *IEEE Access*, **13** (2025.), 35645–35661. https://doi.org/10.1109/ACCESS.2025.3539746
28. J. H. Chang, J. L. Yin, Y. R. Hao, C. X. Gao, STFDSGCN: Spatio-temporal fusion graph neural network based on dynamic sparse graph convolution GRU for traffic flow forecast, *Sensors*, **25** (2025), 3446. https://doi.org/10.3390/s25113446
29. A. Q. Albayati, S. A. J. Altaie, W. N. I. Al-Obaydy, F. F. Alkhalid, Performance analysis of optimization algorithms for convolutional neural network-based handwritten digit recognition, *IAES Int. J. Artif. Intell*, **13** (2024), 563–571. http://doi.org/10.11591/ijai.v13.i1.pp563-571
30. J. Graham, V. S. Sheng, SHAP informed neural network, *Mathematics*, **13** (2025), 849. https://doi.org/10.3390/math13050849
31. UAV Autonomous Navigation Dataset. Available from: https://www.kaggle.com/datasets/ziya07/uav-autonomous-navigation-dataset/data
32. A. V. R. Katkuri, H. Madan, N. Khatri, A. S. H. Abdul-Qawy, K. S. Patnaik, Autonomous UAV navigation using deep learning-based computer vision frameworks: a systematic literature review, *Array*, **23** (2024.), 100361. https://doi.org/10.1016/j.array.2024.100361